Organic Electronics 10 (2009) 815–821

Contents lists available at ScienceDirect

Organic Electronics

journal homepage: www.elsevier.com/locate/orgel

Self-patterning of high-performance thin film transistors

Kuo-Jui Chang [b], Feng-Yu Yang [a,*], Cheng-Chin Liu [b], Meei-Yu Hsu [a], Ta-Chuan Liao [b], Huang-Chung Cheng [b]

[a] Materials and Chemical Laboratories, Industrial Technology Research Institute, 195, Sec. 4, Chung Hsing Road, Chutung, Hsinchu 310, Taiwan
[b] Department of Electronics Engineering and Institute of Electronics, National Chiao Tung University, Hsinchu 300, Taiwan

ARTICLE INFO

Article history:
Received 23 December 2008
Received in revised form 23 March 2009
Accepted 7 April 2009
Available online 14 April 2009

PACS:
73.61

Keywords:
Self-patterning
SAMs
Surface energy
Organic thin film transistors

ABSTRACT

We have developed a technique for the preparation of thin film transistors (TFTs) through the self-patterning of various organic and inorganic materials via solution processing using a wide range of solvents. To obtain selectively self-patterned layers, we treated the oxide dielectric with two-phase patterned self-assembled monolayers of hexamethyldisilazane (HMDS) and octyltrichlorosilane. The conducting polymer poly(3,4-ethylenedioxythiophene) doped with poly(styrene sulfonic acid) in water and the dielectric polymer poly(vinyl phenol) in propylene glycol methyl ether acetate were both selectively deposited and patterned on the HMDS regions with high-quality feature shapes. When source and drain electrodes were patterned on the bottom-gate oxide wafer, we also self-patterned organic and inorganic semiconductors around the channel (HMDS) regions. These TFT devices exhibited moderate to good electronic characteristics. This method has great potential for the economical full solution processing of large-area electronic devices. The selectivity in the patterning phenomena can be understood in terms of surface energy interactions.

1. Introduction

Organic thin film transistors (OTFTs) are attracting much attention for their potential applications in next-generation devices, such as flexible displays, RFIDs, smart cards, electronic paper, sensor arrays, and low-cost disposable electronic devices [1–6]. They exhibit several advantageous features – large areas, low cost, light weight, mechanical flexible, and low-fabricating temperature – that make them preferable to inorganic-based devices; in addition, they can be prepared directly on flexible plastic substrates. During the last two decades, a number of remarkable improvements – in materials development [7–9], the modification of self-assembly monolayers (SAMs) at organic semiconductor–dielectric interfaces [10–13], and device structure engineering [14–16] – have made OTFTs competitive with silicon-based devices. For practical applications, efficient patterning is crucial to the development of electronic devices and circuits. Notably, semiconductors that are not patterned exhibit cross-talk between adjacent devices, parasitic resistance, and gate leakage current (I_G) and drain current (I_D) offsets that are more dramatic than those of patterned systems [17,18]. There are two major approaches that are used to deposit the active semiconductor layer: thermal evaporation and solution processing. Although thermal evaporation through a shadow mask can produce well-ordered patterned films, the throughput is slow and involves expensive vacuum systems. Low-cost solution processing, on the other hand, usually produces non-patterned films that cover the entire substrate. When patterning semiconductor films, which are usually sensitive to oxygen, water, and solvents, common photolithography methods cannot usually be applied directly without a protective capping layer present on top of the semiconductor layer prior to coating of the photoresist. Parylene-C and polyvinylalcohol (PVA) [19–21] and their organic/inorganic bilayers of SiO_2, SiN_x, Al_2O_3, and Al [22] are the most common materials used as protecting layers. Several patterning methods have been developed recently for use in conjunction with solution

* Corresponding author. Tel.: +886 3 5912643; fax: +886 3 5827694.
E-mail address: FengYuYang@itri.org.tw (F.-Y. Yang).

1566-1199/$ - see front matter © 2009 Elsevier B.V. All rights reserved.
doi:10.1016/j.orgel.2009.04.002

processing, including ink-jet printing, screen printing [23], soft lithography [24,25], laser-assisted patterning [26,27], contact printing [28], and self-organization processes [29–33]. Among these methods, self-organization has great potential for use in the fabrication of high-throughput, low-cost electronics without degrading their OTFT performances. For example, Bao et al. [29] reported a microcontact printing (μCP) method for transferring low-molecular-weight siloxane oligomers from PDMS stamps to pattern organic poly(3-hexylthiophene) (P3HT) and poly(vinyl phenol) (PVP) materials via selective wetting/dewetting to fabricate regions with and without oligomers [29]; nevertheless, the interface of the channel region was only the bare surface, lacking a modification layer. Many authors have determined that modification layers present between the dielectric and organic active material are necessary to improve the interfacial adhesion and the film's crystallinity, thereby providing more-stable devices exhibiting higher carrier mobilities [10]. During the preparation of this manuscript, two research groups published self-organization processes featuring the treatment of two modification layers on silicon oxide surfaces [32,33]. Minari et al. [32] reported a surface presenting phenyl-terminated SAMs as channel regions and hexamethyldisilazane (HMDS) units covering the rest of the surface. Small organic molecules that had been drop-cast from toluene solutions were selectively crystallized on the phenyl-presenting SAM regions. Kim et al. [33] coated a hydrophobic fluoropolymer film onto silicon dioxide and then modified the channel regions with HMDS. A soluble pentacene derivative was then self-deposited from a xylene solution onto the channel areas. Although these two initial studies [32,33] appear to have several advantages over simple mono-modification treatment [29–31] the authors studied the patterning of semiconductors in nonpolar solvents only; they did not explore the use of other materials (e.g., conducting polymers, organic gate dielectrics) or other polar and nonpolar solvents. In addition, the origins of the self-organization processes were considered to occur mostly through differences in the water contact angles of the substrates inducing the hydrophilic/hydrophobic properties; there remains much room to provide a more appropriate explanation of these phenomena.

In this study, we developed a new system for the self-patterning of two types of SAMs on silicon dioxide surfaces, with HMDS forming channel regions and octyltrichlorosilane (OTS) covering the remaining areas. We prepared these patterns readily using traditional photolithography processes. In addition to investigating several organic and inorganic semiconductors, we also processed the conducting polymers from aqueous solutions and employed organic gate dielectric materials. We explain the self-patterning phenomena in terms of surface energy differences – rather than the previously reported simple hydrophilic/hydrophobic water contact angle theory.

2. Experimental section

Materials: PVP (M_w = 20,000), PMF (M_w = 511), OTS, HMDS, chlorobenzene, toluene, propylene glycol monomethyl ether acetate (PGMEA), CH_2Cl_2, hexane, and acetone were purchased from Sigma–Aldrich and used without further purification. Regioregular P3HT was purchased from Aldrich and purified through Soxhlet extractions with hexane and CH_2Cl_2 to remove low-molecular-weight chains. 13,6-*N*-sulfinylacetamidopentacene (NSFAAP) and zinc acetate were also obtained commercially from Aldrich and used directly. Poly(9,9-dioctylfluorene-*alt*-bithiophene (F8T2) was purchased from American Dye Source. The PEDOT:PSS water solution (AI4083) was purchased from Bayer.

Device fabrication: We prepared the substrate using the self-patterning process presented in Fig. 1. We employed a silicon wafer presenting thermally grown SiO_2 (d = 100 nm) as the substrate. The source and drain (S/D) Pt/Ti (50 nm/2 nm) electrodes having channel widths and lengths of 1000 and 10 μm, respectively, were prepared using a photolithography/Pt–Ti deposition/lift-off (acetone) process. The entire device surface was treated with HMDS vapor and then cured at 150 °C for 0.5 h, and then the channel regions of the device were covered with photoresist using conventional photolithography processing. The remaining region not covered with the photoresist was treated through O_2 plasma bombardment and then treated with OTS vapor then cured at 100 °C for 0.5 h. Finally, the photoresist was removed to provide a substrate presenting HMDS in the channel regions and OTS over the remaining areas.

Electrical Measurements: All TFT devices arrays in this study, each containing 20 devices were fabricated. To ensure accuracy of data that were collected, we measured at least 10 devices for each array and no significant (<10%) variations were observed from device to device. All *I*–*V* measurements of our OTFT devices were recorded at room temperature under ambient conditions using an Agilent 4156C semiconductor parameter analyzer. The thicknesses of the corresponding films were determined through cross-sectional scanning electron microscopy (SEM). The surface energies of the various SAM surfaces were determined through contact angle measurements using a FACE contact-angle meter (Kyowa Kaimenkagaku Co.) and distilled water and CH_2I_2 as probe liquids.

3. Results and discussion

We employed various solutions of organic and inorganic materials to examine the scope of this self-patterning method; Fig. 2 presents their chemical structures. After depositing a drop of the semiconductor solution [P3HT (5 mg) in dichlorobenzene (1 mL)] onto the HMDS/OTS-presenting S/D electrode-patterned substrate and then decanting the substrate to remove the large droplet, we found that some small droplets remained adhered to the HMDS regions. After the solvent had dried, the resulting films were isolated with finely featured shapes on the HMDS region. Thus, using this approach, we fabricated a bottom gate, bottom contact configuration of the patterned P3HT-OTFT. Fig. 3a displays an optical micrograph of the with uniformly patterned P3HT-OTFT device array. A magnified image of the P3HT-OTFT single device (Fig. 3b)

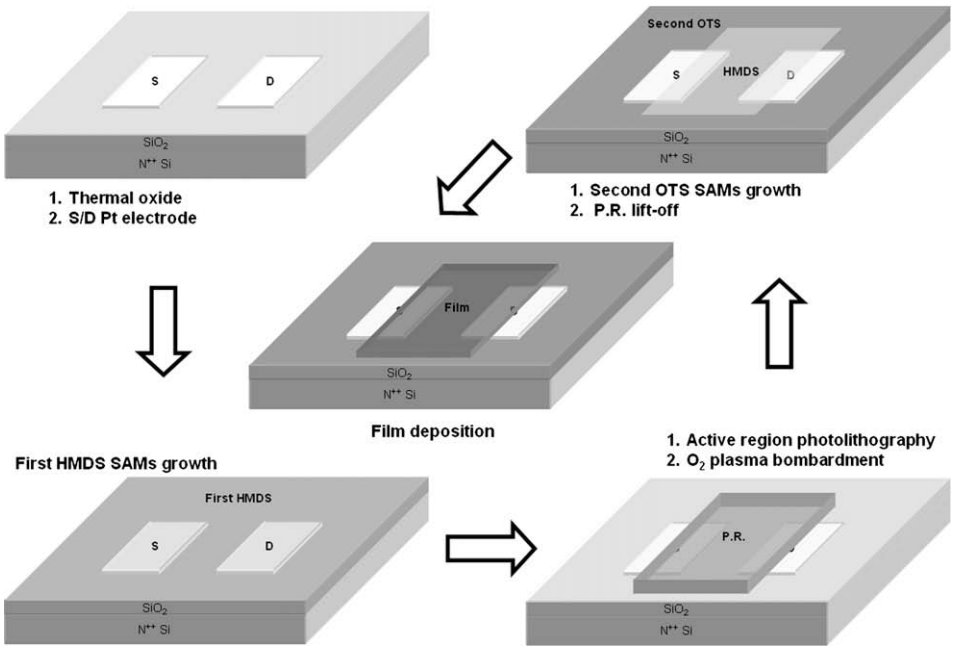

Fig. 1. Schematic procedure used for the self-patterning of OTFTs.

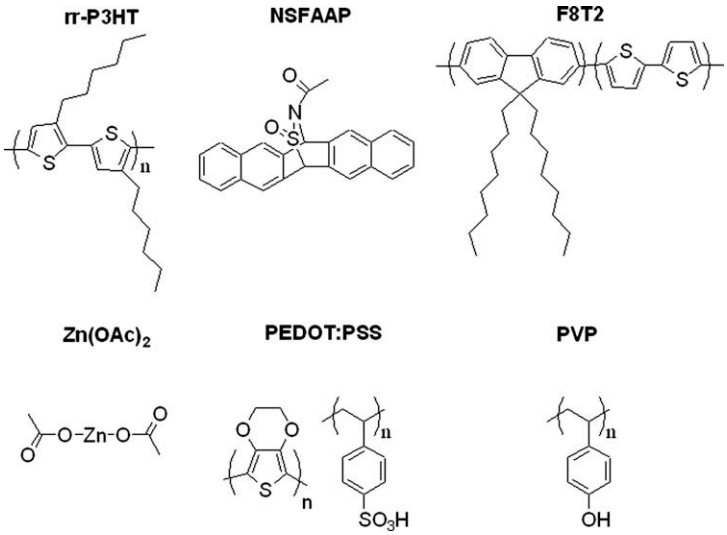

Fig. 2. Chemical structures of the materials used to prepare the patterned organic and inorganic films.

reveals rectangular features (250 μm × 300 μm). In addition, when we used the HMDS/OTS-presenting substrate lacking any S/D electrodes, we formed films of the organic conductor poly(3,4-ethylenedioxythiophene) doped with poly(styrene sulfonic acid) (PEDOT:PSS) from an aqueous solution (Fig. 3c) and of poly(vinyl phenol) (PVP), a commonly used dielectric layer, from a propylene glycol methyl ether acetate (PGMEA) solution (Fig. 3d); these polymers were also well defined in the desired regions, with their films were exhibiting uniformly striped rectangular featured having areas of 100 μm × 1000 μm. Thus, a series of materials could be self-patterned using HMDS/OTS substrates through solution processing with a wide range of solvents.

We used an energy dispersive spectrometer (EDS) to analyze the surfaces of the patterned P3HT-OTFT devices to determine whether any residues or contaminants existed outside the active region after performing the solution deposition process. Before taking SEM photographs, we deposited a thin Pt film to make the substrate conductive. So the Pt signals were observed at both regions. Fig. 4 presents EDS spectra recorded over an active P3HT region and over a P3HT-free region. P3HT has the chemical formula $C_{10}H_{14}S$; we found S and C atom signal distributions

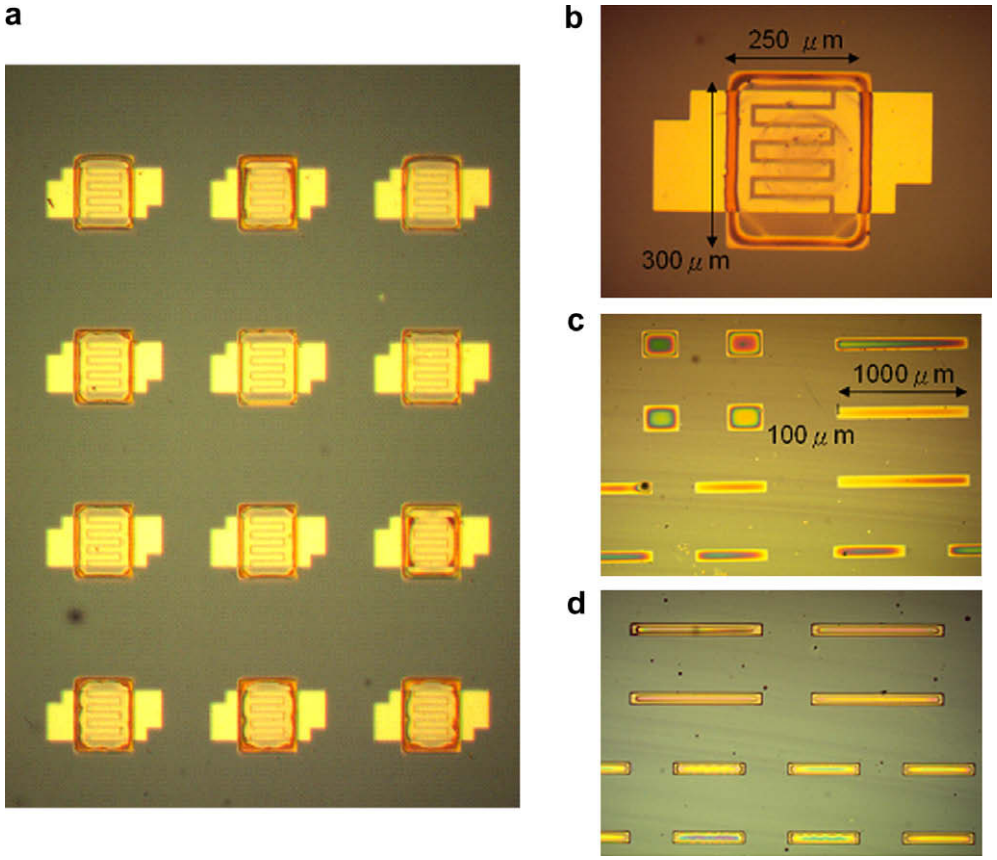

Fig. 3. Optical micrographs of silicon substrates presenting (a) a P3HT-OTFT array, (b) a single P3HT-OTFT device, (c) a PEDOT:PSS array, and (d) a PVP self-patterned array.

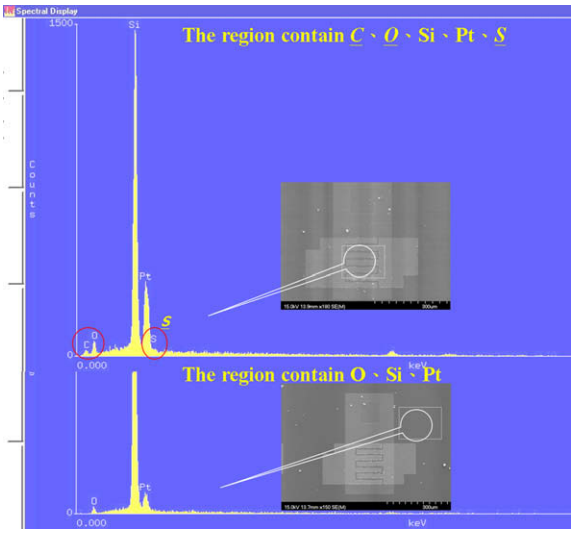

Fig. 4. SEM images and EDS spectra of a P3HT-OTFT device prepared using the self-patterning method.

in the EDS profile of active region, as well as O, Si, and Pt atom signals representing the SiO_2 substrate and the S/D Pt electrodes. In contrast, the EDS profile recorded away from the HMDS region, i.e., the region presenting OTS, reveals signals only for O, Si, and Pt atoms, suggesting that no or non-sufficient P3HT residues or other organic contaminants were present in this area.

In addition to rr-P3HT, we also employed two other organic semiconductors – poly(9,9-dioctylfluorene-*alt*-bithiophene (F8T2; 20 mg in 1 mL of $CHCl_3$), 13,6-*N*-sulfinylacetamidopentacene (NSFAAP; 15 mg in 1 mL of $CHCl_3$) – and one inorganic semiconductor (ZnO precursor solution; zinc acetate-to-ethanolamine molar ratio, 1:1; mixture concentration, 0.375 M in 2-methoxyethanol) to prepare OTFTs using the HMDS/OTS substrates. Again, we found that all of the resulting films exhibited isolated, fine feature shapes located in the HMDS regions, thereby providing bottom gate, bottom contact configurations for their patterned OTFTs. Moreover, we prepared corresponding controlled non-patterned P3HT-OTFT devices to compare their off currents with those of the patterned devices. Fig. 5 presents the electronic characteristics of the OTFT devices; we determined the transfer characteristics of P3HT, F8T2, and pentacene devices by operating the devices at a value of V_{ds} of −40 V and values of V_G ranging from +40 to −40 V and of ZnO device by operating at a value of V_{ds} of 20 V and values of V_G ranging from −10 to 60 V. We define the carrier mobility (μ) and the threshold voltage V_{th} using Eq. (1):

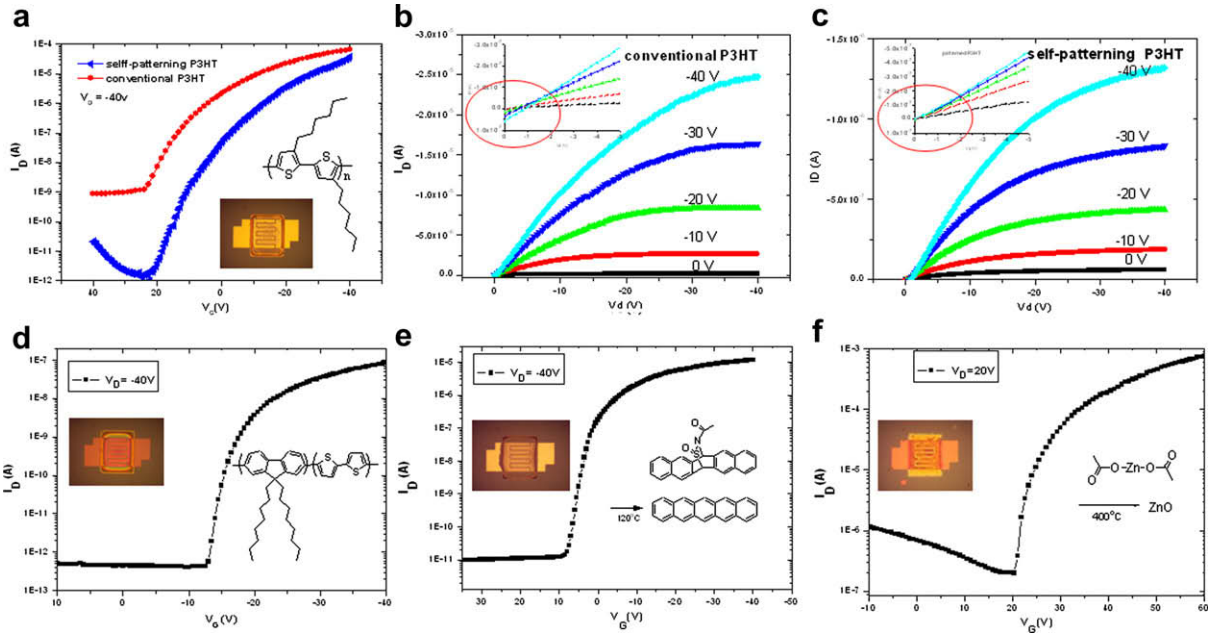

Fig. 5. (a) Transfer curves and (b and c) output curves of P3HT devices prepared on non-patterned and self-patterned semiconductor films. (d–f) Transfer curves of the (d) F8T2, (e) pentacene precursor, and (f) ZnO TFT devices.

$$\sqrt{I_{D,SAT}} = \sqrt{\frac{W\mu C_{ox}}{2L}}(V_G - V_{th}) \quad (1)$$

where $I_{D,sat}$ is the saturated drain current, C_{ox} is the gate capacitance per unit area, W and L are the conducting channel width and length, respectively, and V_G is the applied gate voltage. We extracted the mobilities from the slopes of the linear plots of the square root of the drain current versus the gate voltage. The transfer curve of the non-patterned P3HT-OTFT device (Fig. 5a) exhibited an off current of 10^{-9} A. The on/off ratio, the mobility, and the threshold voltage were 8.9×10^4, 3.2×10^{-2} $cm^2\,V^{-1}\,s^{-1}$, and 8 V, respectively. For the patterned P3HT-OTFT device (also presented in Fig. 5a), the on/off ratio improved dramatically from 8.9×10^4 to 3.8×10^7, with the off current decreasing from 10^{-9} to 10^{-12} A. We suspect that the off current was suppressed effectively as a result of self-patterning. The mobility of the patterned P3HT device decreased only slightly (to 2.6×10^{-2} $cm^2\,V^{-1}\,s^{-1}$) relative to that of the non-patterned device ($3.2 \times 10^{-2}\,cm^2\ V^{-1}\,s^{-1}$). The differences of mobilities caused by patterning of P3HT layer was also found by Jia et al. [17] Fig. 5b and c present the I_D–V_D output characteristics of the non-patterned and self-patterned P3HT-OTFTs, respectively; the insets provide the drain current (I_D) offset, defined as the value of I_D at various gate biases, when the drain voltage was zero [18]. Ideally, the value of the I_D offset would be zero when V_D is zero. For the non-patterned device (Fig. 5b inset), the value of the I_D offset increased when higher gate voltages were applied; the I_D–V_D output curve in the linear region was clearly distorted. On the other hand, the I_D–V_D output curve of the patterned device exhibited an ideal I_D offset (Fig. 5c inset), thanks to the patterning effect of the semiconductors. Note that NSFAAP is transformed into pentacene through thermally degradation, and that ZnO films are formed from zinc acetate during high temperature annealing. Fig. 5d–f display the transfer curves of the F8T2, pentacene, and ZnO TFTs, respectively. The on/off ratio, mobility, and threshold voltage of the F8T2 device were 2×10^5, 2.1×10^{-5} $cm^2\,V^{-1}\,s^{-1}$, and −5 V, respectively; for the pentacene-containing device, these values were 7×10^6, 3.5×10^{-2} $cm^2\,V^{-1}\,s^{-1}$, and 7 V, respectively; for the ZnO-based device, they were 3×10^3, 0.31 $cm^2\,V^{-1}\,s^{-1}$, and 5 V, respectively. Thus, all of these OTFT devices exhibited moderate to good electrical characteristics after performing self-patterning, suggesting that this method has great potential for application to the preparation of large-area, low-cost organic electronic devices.

To determine the origins of the self-patterning effect, we determined the surface energies of the SAM-treated dielectrics by measuring their contact angles for distilled water and CH_2I_2 as probe liquids and employing the geometric mean Eq. (2) [34]:

$$(1 + \cos\theta)\gamma_{pl} = 2(\gamma_s^d \gamma_{pl}^d)^{1/2} + 2(\gamma_s^p \gamma_{pl}^p)^{1/2} \quad (2)$$

where γ_s and γ_{pl} are the surface energies of the sample and probe liquid, respectively, and the superscripts d and p represent the dispersion and polar components of the surface energy, respectively. Table 1 summarizes the contact angles and surface energies of our various SAM-modified surfaces. The surface energies of the active regions (HMDS on SiO_2: 37.4 mJ m^{-2}; HMDS on Pt: 40.7 mJ m^{-2}) of the P3HT-OTFT devices were higher than those of the non-active regions (OTS on SiO_2: 24.5 mJ m^{-2}; OTS on Pt: 31.9 mJ m^{-2}). Because the surface energy is related to the absorbance of the surface, a surface having a high surface energy more readily absorbs the contacting liquid. Fig. 6

Table 1
Contact angles and surface energies of various SAM-modified surfaces.

Surface treatment	Contact angle		Surface energy (dispersion component) γ_s^d (mJ m^{-2})	Surface energy (polar component) γ_s^p (mJ m^{-2})	Surface energy (substrate) γ_s (mJ m^{-2})
	Water(°)	CH_2I_2(°)			
Bare SiO_2	61.5	53.9	32.1	14.6	46.7
Bare SiO_2 + HMDS	74.8	59.4	28.9	8.5	37.4
Bare SiO_2 + O_2 plasma	25.2	43.1	38.0	32.0	70.0
Bare SiO_2 + O_2 plasma + OTS	98.2	69.6	23.1	1.5	24.5
Bare Pt	86.9	40.8	37.2	1.6	40.8
Bare Pt + HMDS	85.2	41.9	38.6	2.1	40.7
Bare Pt + O_2 plasma	87.6	35.8	41.7	1.2	42.8
Bare Pt + O_2 plasma + OTS	95.0	56.0	30.9	1.0	31.9

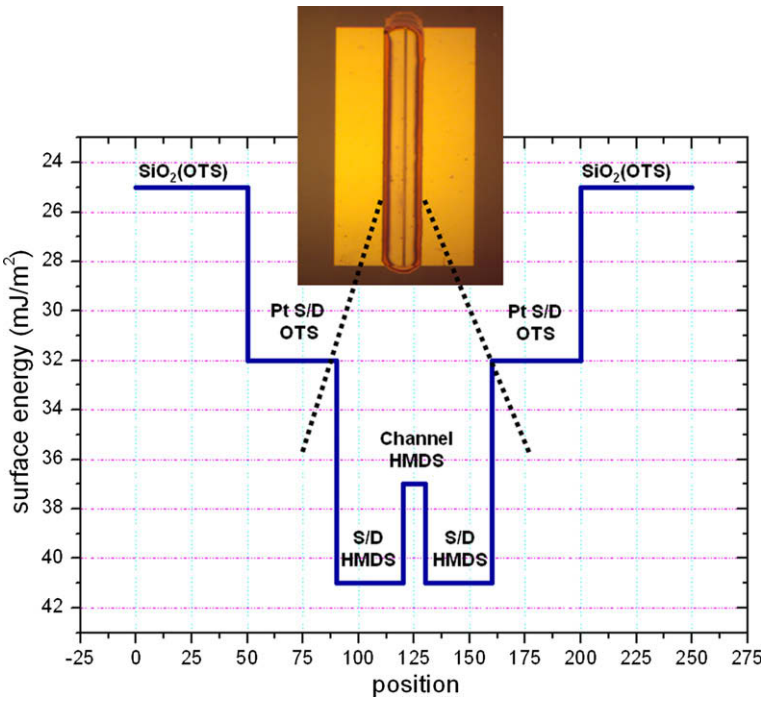

Fig. 6. Surface energy diagram for the OTFT devices.

presents the surface energies of the HMDS/OTS-treated surfaces with S/D Pt electrodes (stripe pattern; W = 500 μm, L = 10 μm) as well as their relative locations. We observe that the contacting liquids more readily adhere to the HMDS surface with its higher surface energy than to the OTS surface with its lower surface energy. When we placed a drop of P3HT in dichlorobenzene onto the device substrate's surface, the droplet selectively wetted/adhered to the HMDS regions and dewetted the OTS regions. After decanting the substrate, the remaining P3HT solution was located (adhered) only on the areas of higher surface energy. As the solvent was evaporated, the P3HT film formed in the desired areas with confined features. The use of contacting liquids of other organic and inorganic semiconductors in either $CHCl_3$ or methoxyethanol, of PEDOT:PSS in aqueous solutions, and of PVP in PGMEA solution was also compatible with this method.

We note that both the HMDS- and OTS-SiO_2 surfaces possessed large water contact angles, i.e., the surfaces are hydrophobic; therefore, aqueous solutions should not adhere to them at all. Indeed, several researchers have reported self-organization processes in which HMDS-SiO_2 [32] and OTS-SiO_2 [30,31] act as dewetting regions. In our case, however, the two HMDS- and OTS-SiO_2 surfaces provided a unique patterning platform for successful solution processing using a wide range of solvents. Therefore, the simple hydrophilic/hydrophobic interactions cannot explain our wetting phenomena. We believe that the surface energy interactions – considering the differences in surface energy of the two SAMs – is more suitable for explaining this self-patterning phenomenon.

4. Conclusions

In summary, we have developed a solution-processable self-patterning method using a two-phase SAM-modified silicon dioxide surface for the deposition of a variety of

organic and inorganic materials from both organic and aqueous solutions. The resulting films were self-patterned in the desired regions with well-defined feature shapes. From analyses of substrates presenting S/D electrodes, all of our self-patterned TFT devices exhibited moderate to good electronic characteristics. This method has great potential for application to the fabrication of large-area, low-cost, fully-solution-processed electronics when combined with mature photolithographic technology for mass production. Surface energy interaction explains this self-patterning phenomenon more suitably than does a simple hydrophilic/hydrophobic interaction.

Acknowledgments

The authors thank the Ministry of Economic Affairs (8351A11410) and the National Science Council (NSC97-2218-E-009-005) of the Republic of China for financially supporting this research.

References

[1] H. Sirringhaus, T. Kawase, R.H. Friend, T. Shimoda, M. Inbasekaran, W. Wu, E.P. Woo, Science 290 (2000) 2123.
[2] L.-L. Chua, J. Zaumseil, J.-F. Chang, E.C.W. Ou, P.K.H. Ho, H. Sirringhaus, R.H. Friend, Nature 434 (2005) 194.
[3] B. Crone, A. Dodabalapur, Y.-Y. Lin, R.W. Filas, Z. Bao, A. LaDuca, R. Sarpeshkar, H.E. Katz, W. Li, Nature 403 (2000) 521.
[4] J.H. Burroughes, D.D.C. Bradley, A.R. Brown, R.N. Marks, K. Mackay, R.H. Friend, P.L. Burns, A.B. Holmes, Nature 347 (1990) 539.
[5] A. Afzali, C.D. Dimitrakopoulos, T.O. Graham, Adv. Mater. 15 (2003) 2066.
[6] A. Afzali, C.D. Dimitrakopoulos, T.L. Breen, J. Am. Chem. Soc. 124 (2002) 8812.
[7] C.D. Dimitrakopoulos, P.R.L. Malenfant, Adv. Mater. 14 (2002) 99.
[8] G. Horowitz, Adv. Mater. 10 (1998) 365.
[9] A. Facchetti, Mater. Today 10 (3) (2007) 28.
[10] S. Kobayashi, T. Nishikawa, T. Takenobu, S. Mori, T. Shimoda, T. Mitani, H. Shimotani, N. Yoshimoto, S. Ogswa, Y. Iwasa, Nat. Mater. 3 (2004) 317.
[11] W.-Y. Chou, H.-L. Cheng, Adv. Func. Mater. 14 (2004) 811.
[12] S.-Z. Weng, W.-S. Hu, C.-H. Kuo, Y.-T. Tao, L.-J. Fan, Y.-W. Yang, Appl. Phys. Lett. 89 (2006) 172103.
[13] Y. Wu, P. Liu, B.S. Ong, T. Srikumar, N. Zhao, G. Botton, S. Zhu, Appl. Phys. Lett. 86 (2005) 142102.
[14] S. Natalie, R.H. Friend, H. Sirringhaus, Science 299 (2003) 1881.
[15] R. Parashkov, E. Becker, S. Hartmann, G. Ginev, D. Schneider, H. Krautwald, T. Dobbertin, D. Metzdorf, F. Brunetti, C. Schildknecht, A. Kammoun, M. Brandes, T. Riedl, H. Johannes, W. Kowalsky, Appl. Phys. Lett. 82 (2003) 4579.
[16] Y.H. Kim, S.M. Han, W. Lee, M.K. Han, Y.U. Lee, J.I. Han, Appl. Phys. Lett. 91 (2007) 042113.
[17] H. Jia, E.K. Gross, R.M. Wallace, B.E. Gnade, Org. Electron. 8 (2007) 44.
[18] H. Jia, G.K. Pant, E.K. Gross, R.M. Wallace, B.E. Gnade, Org. Electron. 7 (2006) 16.
[19] S.H. Han, J.H. Kim, J. Jang, S.M. Cho, M.H. Oh, S.H. Lee, D.J. Choo, Appl. Phys. Lett. 88 (2006) 73519.
[20] L. Zhou, S. Park, B. Bai, J. Sun, S. Wu, T.N. Jackson, S. Nelson, D. Freeman, Y. Hong, IEEE Dev. Lett. 26 (2005) 640.
[21] Y. Wang, H. Cheng, Y. Wang, T. Hu, J. Ho, C. Lee, T. Lei, C. Yeh, Thin Solid Films 491 (2005) 305.
[22] J.S. Lewis, M.S. Weaver, IEEE J. Selected Topics Quantum Electron. 10 (2004) 45.
[23] D.A. Pardo, G.E. Jabbour, N. Peyghambarian, Adv. Mater. 12 (2000) 1249.
[24] Z. Bao, J.A. Rogers, H.E. Katz, J. Mater. Chem. 9 (1999) 1895.
[25] M.L. Chabinyc, A. Salleo, Y. Wu, P. Liu, B.S. Ong, M. Heeney, I. McCulloch, J. Am. Chem. Soc. 126 (2004) 13928.
[26] D.G. Lidzey, M. Voigt, C. Giebeler, A. Buckley, J. Wright, K. Bohlen, J. Fieret, R. Allott, Org. Electron. 6 (2005) 221.
[27] H. Kobayashi, T. Shimoda, H. Kiguchi, World Pat. WO 99/46961, 1999.
[28] C. Kim, P.E. Burrows, S.R. Forrest, Science 288 (2000) 831.
[29] A.L. Briseno, M. Robert, M.M. Ling, H. Moon, E.J. Nemanick, Z. Bao, J. Am. Chem. Soc. 123 (2006) 3880.
[30] H.Y. Choi, S.H. Kim, J. Jang, Adv. Mater. 16 (2004) 732.
[31] A. Salleo, A.C. Arias, Adv. Mater. 19 (2007) 3540.
[32] T. Minari, M. Kano, T. Miyadera, S.D. Wang, Y. Aoyagi, M. Seto, T. Nemoto, S. Isoda, K. Tsukagoshi, Appl. Phys. Lett. 92 (2008) 173301.
[33] S.H. Kim, D. Choi, D.S. Chung, C. Yang, J. Jang, C.E. Park, S.H.K. Park, Appl. Phys. Lett. 93 (2008) 113306.
[34] F.M. Fowkes, in: R.L. Patrick (Ed.), Treatise on Adhesion and Adhesives, vol. 1, Marcel Dekker, New York, 1967, p. 352.